

## **INTERACTION OF ULTRASONIC WAVES AND IMPERFECT ADHESION LAYERS: THE INVERSE PROBLEM**

**Ricardo Leiderman and Arthur M.B.Braga**

*Department of Mechanical Engineering,  
Pontificia Universidade Católica do Rio de  
Janeiro, PUC-Rio  
Rio de Janeiro, RJ, Brazil  
leider@civ.puc-rio.br*

**Paul E. Barbone**

*Department of Aerospace and Mechanical  
Engineering,  
Boston University,  
Boston, Massachusetts, U.S.A.,  
barbone@bu.edu*

### **ABSTRACT**

We discuss the problem of using ultrasound to nondestructively inspect the bond quality of adhesively bonded structural plates. The bond quality is modeled in terms of its effective stiffness. The emphasis here is on the inverse problem: Given a measured ultrasound field, determine the stiffness distribution in the bond. We solve this inverse problem using a combination of the Born approximation and the invariant imbedding technique. Example calculations show the inversion is very accurate for sufficiently weak disbonds, but grows increasingly inaccurate for larger flaws.

### **INTRODUCTION**

Adhesive bonding often offers several advantages over mechanical fasteners. Adhesives can distribute loads without stress concentrations, and their use avoids through holes in the pieces being joined. One drawback of adhesive bonds, however, is the difficulty in determining the bond quality without testing the bond to failure. Much progress has been made in this direction in recent years [1 -4].

One of the key advances in the nondestructive evaluation of bond strength lies in the ability to correlate bond strength with bond stiffness [5]. A mechanism to explain this correlation is the local accumulation of microscopic damage (e.g. microcracks). The damage compromises both the stiffness and the strength of the bond. Thus a measure of the degradation of bond stiffness determines the degree of local damage, which in turn relates to the strength of the bond.

We, as well as others, take advantage of this assumed correlation in our work to develop ways to nondestructively evaluate bond strength using ultrasound. To do so, a well-characterized

incident ultrasound field is used to probe an adhesion interface. The ensuing scattered field is determined by all the properties of the insonified structure, including the quality of the bond.

The particular configuration that we consider below is the following. We assume the incident sound field is a time-harmonic, (i.e. continuous wave) Gaussian beam in 2D. The structure is modeled as a plate of infinite extent in two directions, but finite thickness. In the thickness direction, the plate is layered, representing the adherends to be joined together. Between the adherends are the adhesive layers of interest. We allow the adherends to be anisotropic elastic plates. We assume that we know the properties of the plate in the ideal case that is with perfect bonds. Therefore, we can predict accurately the field scattered by the plate in the absence of flaws. Any deviation between the "measured" scattered field and the idealized scattered field is thus attributed to presence of the flaw. From this deviation, we show below how to recover the local distribution of bond stiffness.

The particular contribution of this paper is the characterization of local defects in the adhesive interface. Other recent contributions are of particular value in measuring the background properties (i.e. the properties of the idealized plate). We show how to recover the bond stiffness as a function of position in the plate.

In this, our first attempt at the inverse problem, we confine our attention to weakly scattering bond imperfections. The weak scattering approximation is made precise through the Born approximation (a regular perturbation expansion). As we show in our examples, the scattering from a bond can be weak either because the imperfection is small in magnitude, or because the imperfection is small in extent. If it is too

large in one or the other, however, the accuracy of the Born approximation breaks down.

The adhesion interfaces tend to be very thin, and therefore a high frequency is required to get a signal that is sensitive to its properties. The use of such high frequencies makes the “forward problem,” the prediction of the sound field scattered by the structure, quite challenging to solve quantitatively. Even certain analytically exact solutions [6] and [7], for example, are known to be so highly sensitive to round off error, that they are unusable at high frequencies. For this reason, we work with the invariant imbedding technique.

The following section contains a description of the mathematical model that we use for the adhesive interface. Following that, we review the invariant imbedding technique and show how to extend it to apply to the current case of interest. This leads directly to the solution of the inverse problem in the Born approximation. We then present some examples and conclude.

#### MODELING INHOMOGENEOUS DEFECT

Baik and Thompson in [8] proposed that when the inspecting wavelength is large compared to adhesion layer thickness, adhesion layers can be modeled as distributed normal and transversal springs, as shown in Figure 1.

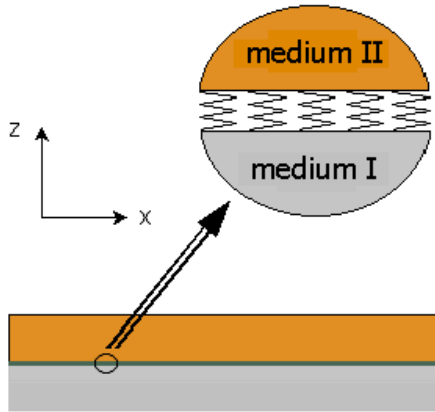


Figure1: The Quasi-Static-Approximation (QSA)

This approximation is known as Quasi-Static-Approximation (QSA) and according to it the boundary conditions between media II and I are:

$$\mathbf{K}(\mathbf{u}'' - \mathbf{u}') = \mathbf{t}'' \quad (1)$$

$$\mathbf{t}'' = \mathbf{t}' \quad (2)$$

Here  $\mathbf{K}$  is a diagonal spring matrix, representing the stiffness of adhesion,  $\mathbf{u}$  is the displacement vector and  $\mathbf{t}$  is the traction vector acting on the  $xy$  plane. Rokhlin and Huang have shown in [9], neglecting inertia and coupling terms, how to determine the spring matrix from the mechanical properties of the adhesion layer.

In practical situations, the thin adhesion layer may suffer degradation due to environmental action or present defects that have been introduced during the manufacturing process. The interaction of elastic waves with such defects will give rise to an acoustic scattered field. Mathematically, this interfacial inhomogeneity may be represented as a perturbation in the original stiffness of adhesion. So the diagonal spring matrix is written as:

$$\mathbf{K} = \mathbf{K}_0 + \varepsilon \mathbf{K}_1(x, y) \quad (3)$$

where  $\mathbf{K}_0$  represents the original stiffness of adhesion and  $\mathbf{K}_1(x, y)$ , a function of  $x$  and  $y$ , represents the inhomogeneity, while  $\varepsilon$  is a dimensionless parameter representing the defect strength.

Expanding the displacement and stress field in a regular perturbation series gives:

$$\mathbf{u} = \mathbf{u}_0 + \varepsilon \mathbf{u}_1 + \varepsilon^2 \mathbf{u}_2 + \varepsilon^3 \mathbf{u}_3 + \dots \quad (4)$$

$$\mathbf{t} = \mathbf{t}_0 + \varepsilon \mathbf{t}_1 + \varepsilon^2 \mathbf{t}_2 + \varepsilon^3 \mathbf{t}_3 + \dots \quad (5)$$

The application of these expansions together with Eq. (3), in Eqs. (1) and (2), leads to a set of boundary conditions that can be grouped according to the power of  $\varepsilon$ , so for  $O(1)$ :

$$\mathbf{K}_0(\mathbf{u}_0'' - \mathbf{u}_0') = \mathbf{t}_0'' \quad (6)$$

$$\mathbf{t}_0'' = \mathbf{t}_0' \quad (7)$$

for  $O(\varepsilon)$ :

$$\mathbf{K}_0(\mathbf{u}_1'' - \mathbf{u}_1') + \mathbf{K}_1(\mathbf{u}_0'' - \mathbf{u}_0') = \mathbf{t}_1'' \quad (8)$$

$$\mathbf{t}_1'' = \mathbf{t}_1' \quad (9)$$

For  $O(\varepsilon^2)$ :

$$\mathbf{K}_0(\mathbf{u}_2^{\text{II}} - \mathbf{u}_2^{\text{I}}) + \mathbf{K}_1(\mathbf{u}_1^{\text{II}} - \mathbf{u}_1^{\text{I}}) = \mathbf{t}_2^{\text{II}} \quad (10)$$

$$\mathbf{t}_2^{\text{II}} = \mathbf{t}_2^{\text{I}} \quad (11)$$

and so on.

By Eqs. (6) and (7) one can see that terms of  $O(1)$  are obtained considering non-defective adhesion layer. In the present work these terms will be referred as *specular* field. It is also shown, in Eqs. (8)-(11), that terms of  $O(\varepsilon^n)$  can be calculated from previously calculated terms of  $O(\varepsilon^{n-1})$ . So an iterative calculation can be applied to solve as many terms as desired. The sum of these terms, terms of  $O(\varepsilon)$  or higher, will be referred as *scattered* field. When the defect's strength is small, the series can be accurately truncated at terms of  $O(\varepsilon)$ , characterizing the Born approximation. The Born approximation is especially useful in the inverse problem solution, as will be seen in the next section.

As seen in Eqs. (8) and (10), terms of the form  $\mathbf{K}_1(\mathbf{u}_n^{\text{II}} - \mathbf{u}_n^{\text{I}})$  can be understood as a stress source, or a surface force acting along the adhesion layer. For notation simplification in next sections we adopt the following representation:

$$\mathbf{K}_1(\mathbf{u}_n^{\text{II}} - \mathbf{u}_n^{\text{I}}) = \varphi_n \quad (12)$$

### RECURSIVE SOLUTION ALGORITHM FOR THE FORWARD PROBLEM

The forward problem consisting of a layered plate immersed in water, in the context of the boundary conditions derived in previous section, is solved with the aid of the invariant imbedding method. By virtue of the perturbation expansion, each term of the series can be computed by considering a laminated plate with perfectly bonded layers, subject to some acoustic sources. The acoustic sources in this case represent "secondary sources" which give rise to the scattered field. So in this section, we consider radiation from a perfectly bonded plate with acoustic sources embedded within it. The problem is shown schematically in Figure 2. The tensors associated with the invariant imbedding method are:  $\mathbf{R}$  - Reflection matrix;  $\mathbf{G}$  - Surface impedance tensor;  $\mathbf{K}_0$  - Diagonal spring matrix representing the original stiffness of adhesion;  $\mathbf{K}_1$  - Diagonal spring matrix representing the non-uniform defect;  $\mathbf{S}$  - Surface tensor which relates stress sources, or equivalent forces, to displacement;  $\mathbf{W}$  - Surface tensor that transports, recursively, stress sources, or equivalent forces, to

plate's top surface. It can be noticed in the figure that roman numerals address each medium (two adherend layers and upper and lower fluid half-spaces) while Arabic numerals as superscripts address each interface. The superscript + indicates position immediately above the adhesive layer.

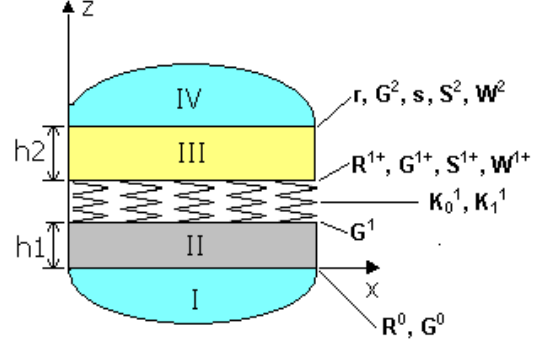


Figure 2: Schematic figure representing the problem and related surface tensors.

The following formulation was developed with the aid of the *upgoing* and *downgoing* formalism. In such formalism plane waves in an homogeneous medium traveling or being attenuated in the positive and negative directions of the vertical ( $z$ ) axis are treated separately and are represented by the subscripts 1 and 2, respectively. Notice that, consequently, in this section these subscripts no longer stand for the term of the series derived in the previous section. According the formalism, displacement and traction vectors, at any coordinate  $z$ , are represented, respectively, by:

$$\bar{\mathbf{u}}(z) = \bar{\mathbf{u}}_1(z) + \bar{\mathbf{u}}_2(z) \quad (13)$$

$$\bar{\mathbf{t}}(z) = \bar{\mathbf{t}}_1(z) + \bar{\mathbf{t}}_2(z) \quad (14)$$

and are related as:

$$\bar{\mathbf{t}}_1(z) = -i\omega\mathbf{Z}_1\bar{\mathbf{u}}_1(z) \quad (15)$$

$$\bar{\mathbf{t}}_2(z) = -i\omega\mathbf{Z}_2\bar{\mathbf{u}}_2(z) \quad (16)$$

where  $\mathbf{Z}_1$  and  $\mathbf{Z}_2$  are the local impedance tensors, which are functions of the mechanical properties of the medium only, while  $\omega$  is the frequency. The bar over  $\mathbf{u}$  and  $\mathbf{t}$  stands for Fourier transform, and indicates that the problem is solved first in

the  $x$ -wavenumber domain. The displacement vectors at different depths are related by:

$$\bar{\mathbf{u}}_1(z2) = \mathbf{M}_1(z2 - z1)\bar{\mathbf{u}}_1(z1) \quad (17)$$

$$\bar{\mathbf{u}}_2(z2) = \mathbf{M}_2(z2 - z1)\bar{\mathbf{u}}_2(z1) \quad (18)$$

where  $\mathbf{M}_1$  and  $\mathbf{M}_2$  are the propagation matrixes of the medium. We note that this formalism is applicable to isotropic as well as to anisotropic media, making the algorithm suitable for both cases.

According to the recursive method proposed here, the *upgoing* displacement vector, at each interface, is defined as:

$$\bar{\mathbf{u}}_1 = \mathbf{R}\bar{\mathbf{u}}_2 + \mathbf{S}\bar{\varphi} \quad (19)$$

or, in the case of the top (fluid /solid) interface, the  $z$  component of the upgoing displacement vector,  $\bar{w}_1$ , in the fluid, is defined as:

$$\bar{w}_1 = r\bar{w}_2 + \mathbf{s} \cdot \bar{\varphi} \quad (20)$$

The traction vector at each interface is defined as:

$$\bar{\mathbf{t}} = -i\omega[\mathbf{G}\bar{\mathbf{u}} + \mathbf{W}\bar{\varphi}] \quad (21)$$

For interfaces situated below the defective one, the tensors  $\mathbf{S}$  and  $\mathbf{W}$  in Eqs. (19)-(21) are considered to be zero.

### The solid/fluid interface

The boundary conditions at this interface are:

$$\bar{\mathbf{t}}^{0-} = \bar{\mathbf{t}}^{0+} \quad (22)$$

$$\bar{\mathbf{t}}^{0-} = -\wp_2 \mathbf{n} \quad (23)$$

$$\bar{\mathbf{u}}^{0-} \cdot \mathbf{n} = \bar{\mathbf{u}}^{0+} \cdot \mathbf{n} \quad (24)$$

where  $\wp$  stands for pressure, and  $\mathbf{n}$  is the unit vector in the  $z$  direction. Notice that here the signs + and - address position immediately above and below the interface respectively. As in the bottom fluid half-space there are only *downgoing* waves (radiation condition), the surface impedance tensor,  $\mathbf{G}^0$ , is defined as:

$$\mathbf{G}^0 = \mathbf{Z}_2^I \quad (25)$$

where  $\mathbf{Z}_2^I$  is the local impedance tensor of the fluid related to the *downgoing* waves defined as:

$$\mathbf{Z}_2^I = \begin{bmatrix} 0 & 0 & 0 \\ 0 & 0 & 0 \\ 0 & 0 & Z_f \end{bmatrix} \quad (26)$$

where  $Z_f$  is defined as:

$$Z_f = \frac{\rho_f c_f^2 (\alpha^2 + \beta^2)}{\omega \beta} \quad (27)$$

and  $c_f$  is the sound speed in the fluid,  $\rho_f$  is the fluid density,  $\alpha$  is the  $x$ -wavenumber and  $\beta$  is the  $z$ -wavenumber. Than it can be shown that:

$$\mathbf{R}^0 = [\mathbf{G}^0 - \mathbf{Z}_1^{II}]^{-1} [\mathbf{Z}_2^{II} - \mathbf{G}^0] \quad (28)$$

### The solid/solid interface

Using the definitions represented by Eqs. (13)-(18), it can be shown that:

$$\mathbf{G}^1 = [\mathbf{Z}_2^{II} + \mathbf{Z}_1^{II} \mathbf{M}_1^{II}(h_1) \mathbf{R}^0 \mathbf{M}_2^{II}(-h_1)]^{-1} [\mathbf{I} + \mathbf{M}_1^{II}(h_1) \mathbf{R}^0 \mathbf{M}_2^{II}(-h_1)] \quad (29)$$

The application of boundary conditions represented by Eqs. (1) and (2) leads to:

$$\mathbf{G}^{1+} = \mathbf{G}^1 \{ [\mathbf{K}_0^1]^{-1} [-i\omega \mathbf{G}^1] + \mathbf{I} \}^{-1} \quad (30)$$

$$\mathbf{R}^{1+} = [\mathbf{G}^{1+} - \mathbf{Z}_1^{III}]^{-1} [\mathbf{Z}_2^{III} - \mathbf{G}^{1+}] \quad (31)$$

$$\mathbf{W}^{1+} = \mathbf{G}^{1+} [\mathbf{K}_0^1]^{-1} \quad (32)$$

$$\mathbf{S}^{1+} = [\mathbf{Z}_1^{III} - \mathbf{G}^{1+}]^{-1} \mathbf{W}^{1+} \quad (33)$$

### The fluid/solid interface

Using the definitions represented by Eqs. (13)-(16) and (19)-(21), it can be shown that:

$$\mathbf{S}^2 = \mathbf{M}_1^{III}(h_2) \mathbf{S}^{1+} \quad (34)$$

$$\mathbf{W}^2 = [\mathbf{Z}_1^{III} - \mathbf{G}^2]^{-1} \mathbf{S}^2 \quad (35)$$

The boundary conditions at this interface are similar to Eqs. (22)-(24), so it can be shown that:

$$r = \frac{Z_s - Z_f}{Z_s + Z_f} \quad (36)$$

where  $Z_s$  is defined as:

$$Z_s = \frac{\det \mathbf{G}^2}{\det \mathbf{G}_{PL}^2} \quad (37)$$

where  $\mathbf{G}^2$  is defined as in (29) and  $\mathbf{G}_{PL}^2$ , a sub-matrix of  $\mathbf{G}^2$ , is defined as:

$$\mathbf{G}_{PL}^2 = \begin{bmatrix} \mathbf{G}^2(1,1) & \mathbf{G}^2(1,2) \\ \mathbf{G}^2(2,1) & \mathbf{G}^2(2,2) \end{bmatrix} \quad (38)$$

Also it can be shown that:

$$s = \left(-\frac{Z_f}{Z_s} - 1\right)^{-1} [\mathbf{W}^2]^T \{[\mathbf{G}^2]^{-1}\}^T \quad (39)$$

#### INVERSE PROBLEM STATEMENT

Here we consider the related inverse problem. As we are concerned primarily with adhesive bond degradation, we suppose that we know the material properties of each layer, and the undegraded adhesive stiffness. Similarly, we assume we know the incident field and, from all other known properties, we can compute the specular field. We remind the reader that we define  $\mathbf{u}_{\text{specular}} \equiv \mathbf{u}_0$  to be the sum of the incident field and its reflection from an ideal plate. By "scattered" field, we mean:

$$\mathbf{u}_{\text{scatt}} = \mathbf{u}_{\text{total}} - \mathbf{u}_{\text{specular}} \quad (40)$$

Thus we get the following problem: Given  $\mathbf{M}^i$ ,  $\mathbf{Z}^i$ ,  $\mathbf{K}_0$ ,  $\mathbf{u}_{\text{specular}}$  and  $\mathbf{u}_{\text{scatt}}$ , find  $\varepsilon \mathbf{K}_1(x)$ .

#### SOLUTION FOR THE INVERSE PROBLEM

To solve this problem, we can use the perturbation solution described above. In particular we note from Eqs. (4) and (1) that

$$\varepsilon \mathbf{u}_1 = \mathbf{u}_{\text{scatt}} + O(\varepsilon^2) + O(\varepsilon^3) + \dots \quad (41)$$

Now, recalling the Born approximation, which neglects terms of  $O(\varepsilon^2)$  or higher, it can be seen that:

$$\varepsilon \mathbf{u}_1 = \mathbf{u}_{\text{scatt}} \quad (42)$$

From Eq. (42), the term  $\varepsilon \boldsymbol{\varphi}_0$  can then be determined by *measuring* the scattered displacement field at the plate's top surface. Specifically, recalling definitions (20) and (21), and using the boundary conditions for the fluid/solid interface, one gets:

$$\varepsilon \bar{\boldsymbol{\varphi}}_0 = [\mathbf{W}^2]^{-1} [-Z_f \bar{\mathbf{W}}_{\text{scatt}}^2 \mathbf{n} - \mathbf{G}^2 \bar{\mathbf{u}}_{\text{scatt}}^2] \quad (43)$$

Equations (8) and (12) show that we can determine  $\varepsilon \mathbf{K}_1$  from  $\varepsilon \boldsymbol{\varphi}_0$ , the effective forcing at  $O(\varepsilon)$ , backsubstituting the  $\mathbf{u}_0$  solution in the defective layer to find the effective bond stiffness. Thus, since  $\mathbf{K}_1$  is diagonal, we get for each value of  $x$ :

$$\begin{aligned} \varepsilon \mathbf{K}_1(1,1) &= \frac{\varepsilon \varphi_0(1)}{\mathbf{u}_{\text{specular}}^{1+}(1) - \mathbf{u}_{\text{specular}}^1(1)} \\ \varepsilon \mathbf{K}_1(2,2) &= \frac{\varepsilon \varphi_0(2)}{\mathbf{u}_{\text{specular}}^{1+}(2) - \mathbf{u}_{\text{specular}}^1(2)} \\ \varepsilon \mathbf{K}_1(3,3) &= \frac{\varepsilon \varphi_0(3)}{\mathbf{u}_{\text{specular}}^{1+}(3) - \mathbf{u}_{\text{specular}}^1(3)} \end{aligned} \quad (44)$$

As are many inverse problems, this is ill conditioned and sensitive to noise in the data. There are two places where that sensitivity can manifest itself. One is evident in equation (43), where we require the inverse of  $\mathbf{W}$ . For some wavenumbers and frequencies, however,  $\mathbf{W}$  is singular or nearly singular. Though  $\mathbf{W}$  is singular, the vector on which  $\mathbf{W}^{-1}$  acts is in its range, and so the right hand side of (43) remains theoretically well defined. When  $\mathbf{u}_{\text{scatt}}$  is replaced by a measured value with some noise, however, some regularization must be applied to ensure that (43) makes sense. The second place that regularization is sometimes needed is when the denominator of (44) vanishes. Again, with noiseless data, the numerator vanishes at the same time as the denominator, making the fraction well defined in the limit. With noisy data, however, regularization is required.

In the numerical results to follow, very high precision numerical data is used as the input data. Therefore, the data is "noiseless" to as high a precision as we can compute and no

regularization was required or applied. Interestingly, we found this to be the case even in the Born approximation. In tests on data with noise artificially added (not shown here), we found sensitivity in the unregularized results as expected. We also found that several standard and simple regularizations could be applied to control that sensitivity. We intend to discuss these topics more fully in a later contribution.

### NUMERICAL RESULTS

Results of the ultrasound inspection simulation of a layered plate immersed in water are presented in this section. The modeled plate, which is considered to be under a plane strain state, is shown schematically in Figure 3. The mechanical properties of its constituent materials are shown in Table 1.

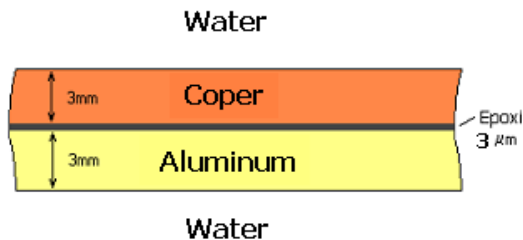


Figure 3: Composite layered plate

Table 1: Properties of constituent materials

| Material | Density (Kg/m <sup>3</sup> ) | P-Wave vel. (m/s) | S-Wave vel. (m/s) |
|----------|------------------------------|-------------------|-------------------|
| Aluminum | 2700                         | 6320              | 3130              |
| Copper   | 8930                         | 4660              | 2660              |
| Epoxy    | 1200                         | 2150              | 1030              |
| Water    | 1000                         | 1480              | 0                 |

For estimate of interfacial stiffness of adhesion, the adhesion layer is considered to have 3µm of thickness and considered to have, when intact, the same mechanical properties of the Epoxy. According Rokhlin and Huang in [9], these interfaces can then be represented as:

$$K_0 = \begin{bmatrix} 0.426 & 0 & 0 \\ 0 & 0.426 & 0 \\ 0 & 0 & 1.846 \end{bmatrix} * 10^{15} Pa / m$$

The considered acoustic incident field is a gaussian wave-beam with about 20cm of length, the frequency is 5.15 MHz and it is incident at an angle of 6.69 degrees. The frequency and incident angle selection is discussed in a recent article written by the authors about the forward problem [10]. The incident field is represented schematically in Figure 4.

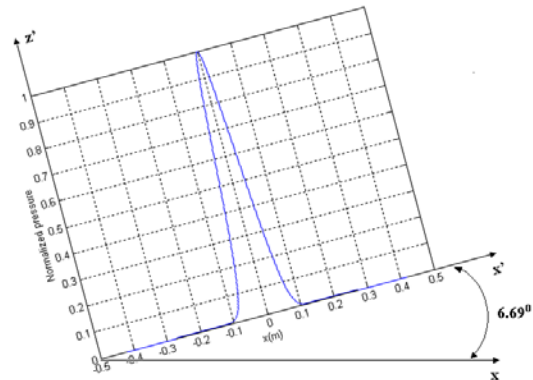


Figure 4 – The incident pressure field.

The modeled defects are represented by Gaussians (in the last case shown in Figure 6 the defect is homogeneous). The simulations are divided in two groups. In the first group the length of defect is the same but its magnitude varies. In the second group the length of defect varies while its magnitude is fixed. In order to emphasize “Kissing bonds” detection, the defects are such that only the x component of the original adhesion stiffness is affected. They are represented in Figures 5 and 6 respectively. The synthetic data representing the scattered field for such scenarios was generated using the method showed in previous sections (for more details see [10]). Several terms of the series were calculated and the convergence was verified. The sum of these terms was considered as the scattered field.

Results related to the first group of defects are presented in Figure 5. Results related to the second group of defects are presented in Figure 6. Notice that the last case presented in the Figure 6 is related to a homogeneous defect.

### DISCUSSION & CONCLUSIONS

We have shown how to characterize localized bond defects through the solution of an inverse acoustic scattering problem. We formulated the inverse problem using a combination of invariant

imbedding and the Born approximation. The invariant imbedding makes the solution of the forward problem robust even at high frequencies. Through example calculations, we demonstrated that high accuracy of the results for weakly scattering bonds, and also the limitations of our method for stronger scattering. The calculations themselves ignore several important features that remain to be considered. Primary among these are

the effects of noise, and the role of uncertainty in the data of the idealized configuration.

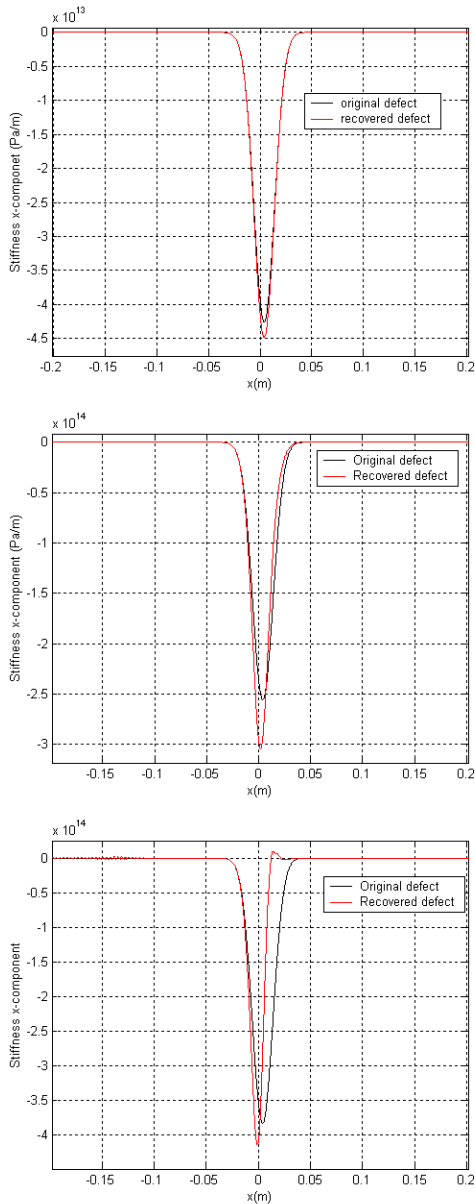


Figure 5: Results of the first group of simulations. The length of the defect remains constant while its magnitude varies.

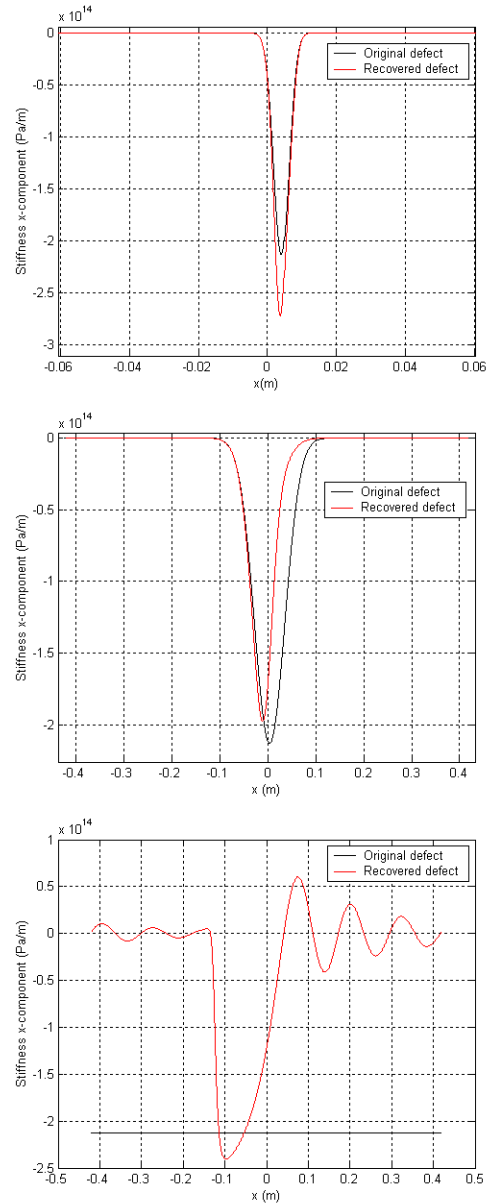


Figure 6: Results of the second group of simulations. The magnitude of the defect remains constant while its length varies.

## REFERENCES

1. A. I. Lavrentyev and S. I. Rokhlin, "Ultrasonic Spectroscopy of Imperfect Contact Interfaces Between a Layer and Two Solids," *J. Acoust. Soc. Am.* **103** (2), p. 657-664 (1998).

2. B. Li, M. Hefetz, and S. I. Rokhlin, "Ultrasonic Evaluation of Environmentally Degraded Adhesive Joints," *Rev. of Prog. in Quantitative* **11**, p. 1221-1228 (1992).
3. L. Singher, Y. Segal, and E. Segal, "Considerations in bond strength evaluation by ultrasonic guided waves," *J. Acoust. Soc. Am.* **96**(4), p. 2497-2505 (1994).
4. T. Pialucha and P. Cawley, "The Detection of a Weak Adhesive/Adherend Interface in Bonded Joints By Ultrasonic Reflection Measurements," *Rev. of Prog. in Quantitative NDE* **11**, p. 1261-1266 (1992).
5. Y.C. Angel and J.D. Achenbach, "Reflection and transmission of elastic waves by a periodic array of cracks," *J. Appl. Mech.* **52**, p. 33-41 (1985).
6. W.T. Thomson, "Transmission of elastic waves through a stratified solid medium," *J. Appl. Phys.* **21**, p.89-93 (1950).
7. N.A. Haskell, "The dispersion of surface waves on multilayered media," *Bulletin of the Seismological Society of America* **43**, p.17-34 (1953).
8. J. M. Baik and R. B. Thompson, "Ultrasonic Scattering from Imperfect Interfaces: A Quasi-Static Model," *J. NDE.* **14**, 177-196 (1984).
9. S. I. Rokhlin and W. Huang, "Ultrasonic Wave Interaction With a Thin Layer Between Two Anisotropic Solids," *J. Acoust. Soc. Am.* **92**, 1729-1742 (1992).
10. R. Leiderman, P. Barbone and A.M.B. Braga "Study of the scattering of ultra-sonic waves by defective adhesion interfaces," *J. Acoust. Soc. Am.* on review.